

This is the accepted manuscript made available via CHORUS. The article has been published as:

Integral cross section measurement of the  
 $^{235}\text{U}(n,n^{\prime})^{235\text{m}}\text{U}$  reaction in a pulsed reactor

G. Bélier, E. M. Bond, D. J. Vieira, N. Authier, J. A. Becker, D. Hyneck, X. Jacquet, Y. Jansen,  
J. Legendre, R. Macri, V. Méot, and P. Romain

Phys. Rev. C **91**, 044605 — Published 8 April 2015

DOI: [10.1103/PhysRevC.91.044605](https://doi.org/10.1103/PhysRevC.91.044605)

# Integral Cross Section Measurement of the $^{235}\text{U}(n,n')^{235m}\text{U}$ Reaction in a Pulsed Reactor

G.Bélier<sup>1</sup>, E.M.Bond<sup>2</sup>, D.J.Vieira<sup>2</sup>, N.Authier<sup>4</sup>, J.A.Becker<sup>3</sup>, D.Hyneck<sup>4</sup>, X.Jacquet<sup>4</sup>, Y.Jansen<sup>4</sup>, J.Legendre<sup>4</sup>,  
R.Macri<sup>3</sup>, V.Méot<sup>1</sup>, P. Romain<sup>1</sup>

<sup>1</sup>Commissariat à l'Energie Atomique et aux Energies Alternatives, DAM DIF, F-91297 Arpajon, France

<sup>2</sup>Los Alamos National Laboratory, Los Alamos, NM 87545, USA

<sup>3</sup>Lawrence Livermore National Laboratory, Livermore, CA 94550, USA

<sup>4</sup>Commissariat à l'Energie Atomique et aux Energies Alternatives, DAM, VALDUC, F-21120 Is-sur-Tille, France

The integral measurement of the neutron inelastic cross section leading to the 26 minutes  $^{235m}\text{U}$  isomer in a fission-like neutron spectrum is presented. The experiment has been performed at a pulsed reactor, where the internal conversion decay of the isomer was measured using a dedicated electron detector after activation. The sample preparation, efficiency measurement, irradiation, radiochemistry purification and isomer decay measurement will be presented. We determined the integral cross section for the  $^{235}\text{U}(n,n')^{235m}\text{U}$  reaction to be  $1.00 \pm 0.13$  b. This result supports an evaluation performed with TALYS-1.4 code with respect to the isomer excitation as well as the total neutron inelastic scattering cross section.

## INTRODUCTION

In the application of nuclear fission all of the contributing processes have to be accurately known in order to calculate an assemblies' reactivity. Usually, it is assumed that the fissioning nuclei are in their ground state. But in some situations, excited states need to be considered and the population of these excited states leads to other reaction channels that can change system behavior. In the case of  $^{235}\text{U}$ , the fission cross section for the first excited state, the 26 minutes isomer, exceeds that of the ground state fission cross section by a factor  $\sim 2$  at thermal neutron energies [1]. At higher energies (up to  $\sim 300$  keV) calculations predict the fission cross section for the isomer to be 20-50% smaller than that of the ground state [2]. Hence there is high interest in determining the excitation and fission properties of the  $^{235m}\text{U}$  isomer.

In 2000 the excitation of the isomer by electromagnetic processes in hot dense plasmas was investigated experimentally [3], but no excitation was observed. Calculations [3] indicated that neutron inelastic scattering would be an effective mechanism for populating the isomer, but no measurement has been made until now. Only the total inelastic cross section has been measured in 4 experiments [4,5,6,7]. Fig. 1. shows the experimental data along with an evaluation performed with the TALYS-1.4 code [8]. These measurements have large uncertainties, both in the cross section and the neutron energy, for the three highest energy points. Most notable is a large disagreement between the evaluation and the lowest energy data point at  $\sim 1$  MeV. The neutron inelastic scattering was also studied by the  $(n,n'\gamma)$  technique at the LANSCE/WNR facility [9] at neutron energies above 4.09 MeV, and at the IRMM/GELINA facility [10] from 0.3 to 9.4 MeV. Although the measured partial  $\gamma$ -production cross sections have small uncertainties, the deduced total inelastic scattering cross section uncertainty is large because the  $\gamma$  cascade is very fragmented, with the most intense  $\gamma$ -line representing only 10 % of the

theoretically estimated total cascade strength [9]. In this context the measurement of the isomer production cross section is also important in constraining the total inelastic scattering cross section.

In this article we report on the measurement of the integral neutron inelastic scattering cross section leading to the  $^{235m}\text{U}$  isomer. The experiment was performed at the pulsed critical reactor CALIBAN (located at the CEA/VALDUC laboratory in France), that has a fission-like neutron spectrum in its central cavity. The number of isomeric atoms produced in an irradiation was measured with a dedicated electron detector specifically designed for the detection of low-energy  $^{235m}\text{U}$  conversion electrons.

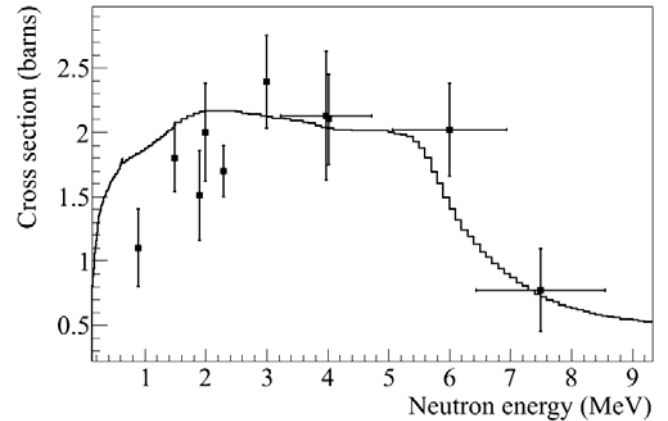


Fig. 1. Total neutron inelastic cross section. The experimental data points are taken from references [4,5,6,7]. The line is an evaluation performed with the TALYS-1.4 code [8].

## II. EXPERIMENT OVERVIEW

The  $^{235m}\text{U}$   $1/2^+$  isomer decays to the  $7/2^-$  ground state by an E3 transition. Due to this high multipolarity and very low

excitation energy ( $E^*=76.8$  eV), this transition is completely converted. The outmost electron shells involved in this decay have binding energies ranging from 4.6 to 44 eV, so that the emitted electrons have a maximum energy of 72.2 eV. Moreover given this very low transition energy, the isomer half-life is very dependent on the chemical environment. Reference [11] has shown a 10 % change in the half-life depending on the oxidation state of the uranium atom. This work has also shown that the half-life depends on the metal in which the isomer is implanted [12]. The common adopted value for the half-life is 26 minutes. For this experiment where the number of  $^{235m}\text{U}$  isomers produced by neutron inelastic reactions is determined by conversion electron counting, the chemical dependence of isomer half-life is an extra uncertainty that must be studied and taken into account. Another complication is the very low energy of the emitted conversion electrons which have a short interaction length of  $\sim 1$  nm ( $\sim 1 \mu\text{g}\cdot\text{cm}^{-2}$  assuming a density  $\rho \sim 10 \text{ g}\cdot\text{cm}^{-3}$  for electroplated U) compared to the electroplated sample thickness ( $\sim 4 \mu\text{g}\cdot\text{cm}^{-2}$ ). Hence the energy spectrum coming out of the sample is highly degraded and no spectroscopy can be done on these electrons. Thus the only observable that can be used to identify the isomer is its half-life. In this respect the determination of the isomer half-life is of prime importance, while the measurement of the isomer detection efficiency and background characterization are essential in determining the neutron inelastic cross section leading to the isomer.

The experiment was performed by irradiating samples in the pulsed reactor CALIBAN [13]. The integrated flux in one ‘shot’ is typically  $3 \times 10^{14} \text{ n}\cdot\text{cm}^{-2}$ . Uranium samples of isotope-enriched  $^{235}\text{U}$ ,  $^{236}\text{U}$ , and  $^{238}\text{U}$  and various blank samples were used to measure the isomer and to characterize the background.

	$^{233}\text{U}$	$^{234}\text{U}$	$^{235}\text{U}$	$^{236}\text{U}$	$^{238}\text{U}$
	(Atomic %)				
$^{235}\text{U}$	0.0001	0.0342	<b>99.84</b>	0.0249	0.1052
$^{236}\text{U}$	0.082	-	0.205	<b>99.68</b>	-
$^{238}\text{U}$	-	0.0054	0.7204	-	<b>99.2742</b>

Table I. Isotopic content of the isotope-enriched uranium samples.

### III. SAMPLE PREPARATION AND FISSION PRODUCT REMOVAL CHEMISTRY

The uranium samples were prepared from solutions that were dried dropwise (stippled) onto Ti backing foils. After irradiation, the uranium was dissolved off of the backing foil and radio-chemically processed to remove fission products. The samples were then electroplated onto a stainless steel disk or a fresh Ti backing foil and then counted. The time from the end of irradiation to the start of counting, hereafter called the ‘cooling time’, was typically 90 minutes. The

isotopic content of the enriched uranium samples, as determined by mass spectroscopy, are given in Table I.

The radiochemical separation, used to remove many of the fission products, was developed at Los Alamos National Laboratory. The separation is based on the extraction chromatographic resin UTEVA, which has a very high affinity for hexavalent uranium and hence can be used to separate uranium from many other elements [14,15]. The radiochemical separation was tested prior to isomer measurements using uranium foils that were irradiated in the GODIVA IV critical assembly [16] at Los Alamos National Laboratory. In a typical radiochemistry development run, a 28 mg foil of highly enriched  $^{235}\text{U}$  was irradiated at GODIVA IV, transported to the radiochemical lab, dissolved in nitric acid, dried, and then redissolved in  $3\text{M HNO}_3 + 0.001 \text{ M HF}$ . The fission products were removed from the uranium using a column containing 2 mL UTEVA resin that had been prewashed with  $3 \text{ M HNO}_3$  and  $3 \text{ M HNO}_3 + 0.001 \text{ M HF}$ . One milliliter of the uranium solution was placed onto the column, followed by rinses of  $5 \text{ mL } 3 \text{ M HNO}_3 + 0.001 \text{ M HF}$  and  $7 \text{ mL } 5 \text{ M HCl}$ . The uranium was subsequently eluted with  $5 \text{ mL } 0.02 \text{ M HNO}_3$ . In Table II we list the separation factors determined for a number of fission products that were observed by gamma spectroscopy using HPGe detectors before and after the separation. In addition, there were a number of isotopes that were observed in the solution prior to the separation, but were not observed following the separation. The separation factors for most of the elements that were observed, were quite good, particularly for Group 1 and 2 elements, and the lanthanides, based on the  $^{143}\text{Ce}$  data. (Noble gas species were released upon dissolution.)

Element	Measured Isotope	$T_{1/2}$	Separation factor
Tc	$^{101}\text{Tc}$	14.2 min	$6300 \pm 1100$
I	$^{135}\text{I}$	6.57 h	$430 \pm 190$
Te	$^{133m}\text{Te}$	55.4 min	$330 \pm 90$
	$^{132}\text{Te}$	3.20 h	$280 \pm 80$
	$^{134}\text{Te}$	41.8 min	$280 \pm 40$
Zr	$^{97}\text{Zr}$	16.8 h	$140 \pm 10$
Sb	$^{131}\text{Sb}$	23.0 min	$120 \pm 30$
	$^{130}\text{Sb}$	39.5 min	$100 \pm 20$

Table II. Summary of measured chemical separation factors (=yield after radiochemistry/yield before radiochemistry) for selected fission products from  $^{235}\text{U}$  samples irradiated in the Godiva IV critical assembly at Los Alamos National Laboratory.

From this work, it is expected that similar, if not improved, separation factors would be obtained with the smaller uranium samples ( $7\text{--}20 \mu\text{g}$  instead of 28 mg) used in the  $^{235m}\text{U}$  measurements. For such small samples, we were able to reduce the amount of UTEVA resin used as well as the solution volumes to reduce the separation time. The

separation procedure used for the samples described in this paper is as follows: The uranium sample was dissolved off the backing material in 1.0 mL 3M HNO<sub>3</sub> + 0.001 M HF; this solution was then poured through a column containing 0.5 mL UTEVA resin. The column was rinsed with an addition of five aliquots of 0.5 mL 3 M HNO<sub>3</sub> + 0.001 M HF, followed by five aliquots of 0.5 mL 5 M HCl. The uranium was then eluted with five 0.5 mL aliquots of 0.01 M HCl directly into an electrodeposition cell and a deposit was prepared using the ammonium sulphate method [17]. Typical separation times where ~30 minutes and electroplating times where ~10 minutes.

#### IV. DETECTION SYSTEMS

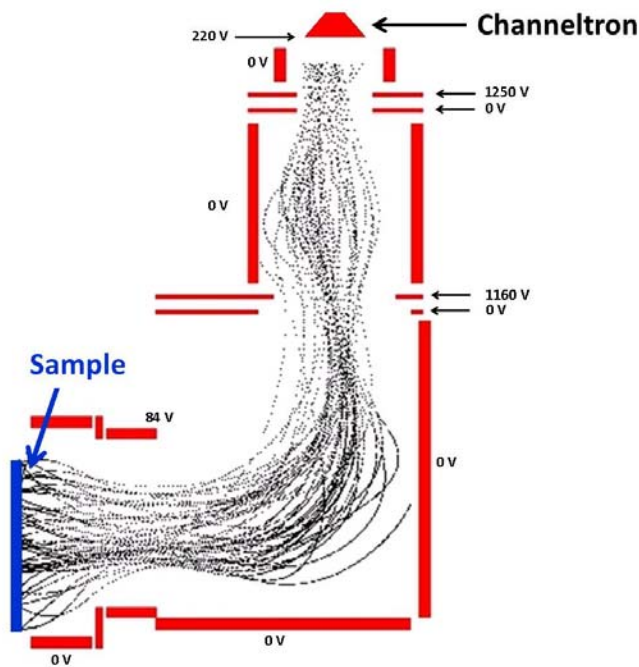


Fig. 2. (Color online) Schema of the electrostatic deflecting electron spectrometer.

A dedicated electron detector has been built for the measurement of the low-energy conversion electrons from the decay of <sup>235m</sup>U (Fig. 2). It is based on an electrostatic deflecting system and a channeltron electron multiplier (Photonics X9551BL). The electrostatic electrodes deflect and accelerate the electrons from a few electron Volts (as emitted from the sample) to 1.5 keV at the entrance of the channeltron. It also focuses the electrons from a 5 cm<sup>2</sup> sample size onto the channeltron whose entrance area is 2.5 cm<sup>2</sup>.

In Fig. 3. the calculated transmission efficiency from the sample to the channeltron is presented. Since the converted electron energies are highly degraded coming out of the sample (due to the short interaction length mentioned above), this apparatus is well suited to the <sup>235m</sup>U isomer decay measurement. This electron spectrometer was originally

developed for a search of the <sup>235m</sup>U isomer excitation in a high-temperature, laser-driven plasma [3].

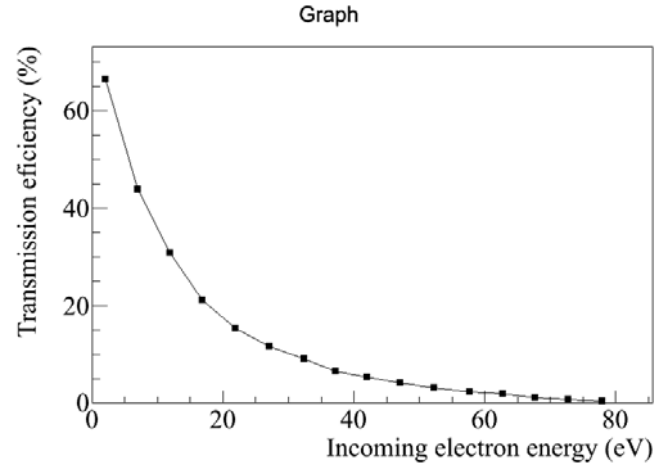


Fig. 3. Calculated electron transmission curve.

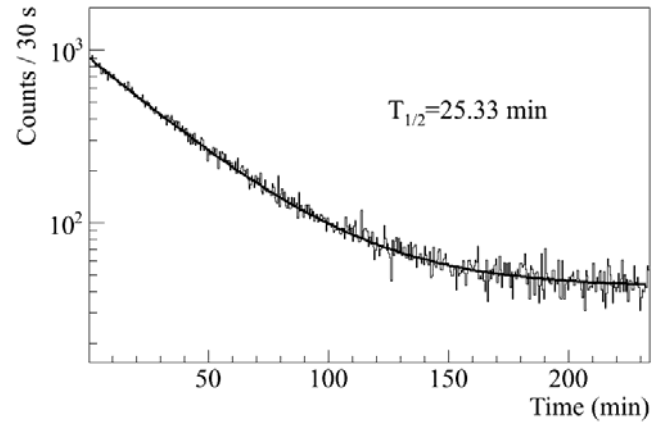


Fig. 4. A typical time spectrum showing the <sup>235m</sup>U isomer decay. The black line is the result of the fit of an exponential decay plus a constant background, from which a half-life of 25.33 minutes was obtained.

In order to minimize the time needed for a sample to be introduced into the electron spectrometer, a vacuum interlock system was used. Using a high-capacity cryo-pump only a few minutes was needed to install the sample, achieve adequate vacuum ( $<10^{-3}$  Pa), bias the channeltron, wait for the dark current to comedown and begin the electron counting. The signal from the channeltron was amplified by an Ortec 113 preamplifier and then shaped by a Tennelec TC244 amplifier. The data acquisition system is based on the ADC 7074 NIM module from Fast Comtec which was linked by a multi-parameter MPA-3 interface to a PC computer. This system time-stamps every event, so that a time spectrum can be constructed. In this experiment two-dimensional histograms were built from the measured pulse height amplitude and time parameters. The time spectrum was

binned in 30 s intervals. Fig. 4 shows a typical time spectrum obtained with a  $^{235}\text{U}$  isomer sample prepared for an efficiency measurement (see below). The black line is the result of the fit of an exponential decay plus a constant background.

The uranium mass of each sample was determined by alpha counting using an  $\alpha$  spectrometer (Eurisy Mesures - EM 7184). It included a passively ion-implanted silicon detector (EM IP 450). The spectrometer detection efficiency was determined by the use of a calibrated alpha source whose total activity was 459  $\alpha/\text{s}$  with an uncertainty of 3 % at the  $2\sigma$  confidence level. This calibrated source contained 3 isotopes,  $^{239}\text{Pu}$ ,  $^{241}\text{Am}$  and  $^{244}\text{Cm}$ , in roughly equal activities so that the system was calibrating in energy as well as efficiency. A small solid angle correction was applied to the measured efficiency in order to take into account the diameter difference between the calibrated source (15 mm) and the  $^{235}\text{U}$  samples (19 mm). This correction ranged from 4.4% for the closest counting distance to 0.3% for the farthest shelf. The obtained spectra were analyzed with the A&M visu  $\alpha$  software [18]. The data analysis consisted of assigning as many  $\alpha$ -peaks as possible to known isotopes in the first step. In a second step, the number of counts for each isotope was deduced from the total counts in the spectra above a fixed threshold and ratioed according to the isotopic content of each target material given in Table I. Finally the masses were calculated by using the calibrated detection efficiency and known branching ratios and half-lives [19].

Irradiated samples were  $\gamma$  counted using three separate and calibrated HPGe detectors. Two of them were devoted to the counting of irradiated uranium and blank samples. The third counter was dedicated to integral flux measurements obtained from indium foils that were co-irradiated with the uranium (or blank) samples. The  $^{115}\text{In}(n,n')^{115\text{m}}\text{In}$  ( $T_{1/2}=4.485$  h,  $E_\gamma = 497$  keV) monitor reaction was used to measure the neutron fluence for each shot. In some cases, the amount of  $^{99}\text{Mo}$  produced by fission in the uranium sample itself could be measured, but because of the small sample masses, the counting statistics were relatively poor (with uncertainties of 10-23 %). These gamma detectors were energy and efficiency calibrated using sources of  $^{152}\text{Eu}$  and  $^{133}\text{Ba}$  whose activity were known to a precision of 2% at the  $1\sigma$  confidence level. (Hereafter all uncertainties are given at the  $1\sigma$  confidence level.) Counting statistics for the indium monitor reaction yielded uncertainties of 1-2 %.

## V. ELECTRON DETECTION EFFICIENCY

In order to characterize the  $^{235\text{m}}\text{U}$  detection efficiency, samples of different masses were prepared and traced with a known amount of isomer obtained by  $\alpha$ -recoil collection from an electrodeposited  $^{239}\text{Pu}$  mother source. The  $^{235}\text{U}$  recoils were implanted into a 1000 Å thick NaCl deposit that was placed 2 mm from the Pu source (100% of  $^{239}\text{Pu}$  alpha decay leads to the population of  $^{235\text{m}}\text{U}$ ). Isomer collections

were done for at least 2 hours under vacuum. The salt deposit was then dissolved off of the backing material using a 0.1 M nitric acid and electroplated with a known amount of  $^{235}\text{U}$  that was added. The  $^{239}\text{Pu}$  mother source had an activity level of  $A_{239}=(2.27\pm0.07)\times10^4$  Bq. This mother source was also traced with  $^{241}\text{Pu}$   $A_{241}=(2.4\pm1)\times10^6$  Bq which was co-deposited with  $^{239}\text{Pu}$  and was used to measure the collection efficiency. Since  $^{241}\text{Pu}$  has a small probability ( $2.45\times10^{-3}$  %) to decay by alpha emission, it produces  $^{237}\text{U}$   $\alpha$ -recoils. The number of collected recoils was determined by  $\gamma$  spectrometry. However because of the low  $^{237}\text{U}$  activity levels collected, these samples were counted close to the detector. The gamma detection efficiency was corrected for summing effects by making separate measurements of the  $^{239}\text{Pu}$ - $^{241}\text{Pu}$  mother source at different distances from the Ge detector. An  $\alpha$ -recoil collection efficiency of  $\varepsilon_c=0.31\pm0.03$  was determined. This value agrees well with the calculated collection solid angle of 0.31. In order to know the exact amount of isomer in the final sample, the electroplating efficiency  $\varepsilon_p$  also has to be known. It is determined from the ratio of the final sample  $^{235}\text{U}$  mass to the  $^{235}\text{U}$  mass added in the solution. The total yield is then obtained by multiplying the collection efficiency, by the plating efficiency. The number of  $^{235\text{m}}\text{U}$  isomers in the prepared sample is finally obtained from this yield and from the collection duration.

For the calibration of the  $^{235\text{m}}\text{U}$  conversion electron detection efficiency, several samples were made by collecting a known amount of  $^{235\text{m}}\text{U}$   $\alpha$ -recoils from the  $^{239}\text{Pu}$ - $^{241}\text{Pu}$  mother source, adding varying amounts of  $^{235}\text{U}$  (which were orders of magnitude larger than that collected as  $\alpha$ -recoils from the source), and electroplated onto a backing foil. A conversion electron decay spectrum (as exemplified in Fig. 4.) was then measured.

Backing Material	Sample form	Half-life (min)
Al	Implanted	26.76 $\pm$ 0.04
Ti	Implanted	27.4 $\pm$ 0.7
Ti	Deposited	25.46 $\pm$ 0.04
Pt	Deposited	26.37 $\pm$ 0.05
Ag	Implanted	25.7 $\pm$ 0.2
NaCl	Implanted	29.01 $\pm$ 0.24
Stainless steel	Deposited	25.62 $\pm$ 0.11

Table III. Measured  $^{235\text{m}}\text{U}$  half-lives determined for  $\alpha$ -recoil implanted samples or for electrodeposited samples involving different backing materials. The half-life uncertainties are statistical only. Systematic uncertainties associated with the data acquisition system clock are considered negligible.

The decay data was fitted using the following function:

$$f(t) = P_1 + P_2 e^{-\ln(2)t/T_{1/2}} \quad (1)$$

where  $P_1$  is the amplitude of the long-lived (effectively constant at our time scale) background coming from

secondary electrons associated with the alpha decay of  $^{235}\text{U}$  and the channeltron dark current and  $P_2$  and  $T_{1/2}$  are the amplitude and half-life of  $^{235m}\text{U}$ , respectively. Because of the chemical effect that influences the isomer half-life, as mentioned earlier, several samples deposited on a variety of backing materials were prepared and their decay spectra measured. The results are given in Table III.

The amplitude  $P_2$  of the isomer decay component is then used to calculate the isomer conversion electron detection efficiency using the following formula:

$$\varepsilon_e = \frac{P_2}{30 \times A_{\text{Pu}} \times \varepsilon_p \times \varepsilon_c} \times \frac{e^{-\frac{t_{\text{cool}}}{\tau_1}}}{1 - e^{-\frac{t_{\text{coll}}}{\tau_2}}} \quad (2)$$

where  $A_{\text{Pu}}$  is the  $^{239}\text{Pu}$  activity of the mother source,  $\varepsilon_p$  is the electroplating efficiency,  $\varepsilon_c$  is the collection efficiency, as mentioned above.  $t_{\text{cool}}$  and  $t_{\text{coll}}$  are the cooling and collection periods, respectively, and  $\tau_1$  is the averaged isomer lifetime during sample cooling and  $\tau_2$  the lifetime in sodium chloride during the recoil collection period.

Because of the half-life chemical dependence effect, we divided the cooling time correction into three parts according to amount of time that the uranium was implanted in NaCl, in solution during electroplating, and as a deposit on the backing material. Thus the cooling correction term becomes

$$e^{-\frac{t_{\text{cool}}}{\tau_1}} = \prod_{i=1}^3 e^{-\frac{t_i}{\tau_i}}$$

Where  $t_i$  and  $\tau_i$  are the measured duration and the isomer lifetimes, respectively, in each medium, as listed in Table III. We used a 15 second timing uncertainty for each period and an aqueous phase half-life of  $25 \pm 2.5$  minutes. This aqueous phase half-life uncertainty reflects the variation observed in this work, as well as that reported by Nève de Mévergnies et al. [11].

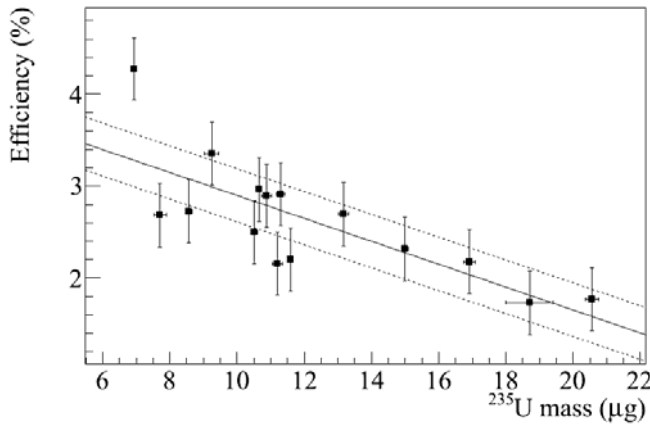


Fig. 5. The  $^{235m}\text{U}$  isomer detection efficiency against the  $^{235}\text{U}$  mass for each sample is plotted. The box size around each data point represents the errors associated with that

sample measurement. The solid line is a linear fit to the data and the dotted lines represent the  $\pm 1\sigma$  limits.

In this study samples with  $^{235}\text{U}$  masses ranging from 1 to 20  $\mu\text{g}$  were electroplated over a diameter of 1.9 cm (as for the CALIBAN measurements). However since for low-mass samples the measured efficiencies had large uncertainties, only samples with masses between 7 and 20  $\mu\text{g}$  were retained. The results of this study are shown in Fig. 5, where the isomer detection efficiency is plotted against the total mass of  $^{235}\text{U}$  in each sample. A linear fit to the data (see Eq. 3) produced a reduced chi square of 1.06 with intercept and slope values of  $\varepsilon_1 = 4.14 \pm 0.3\%$  and  $\varepsilon_2 = -0.125 \pm 0.03\%/\mu\text{g}$ . Hence the isomer detection efficiency is given by:

$$\varepsilon_{\text{isomer}} = \varepsilon_1 + \varepsilon_2 \times m \quad (3)$$

where  $m$  is the  $^{235}\text{U}$  mass of the sample given in micrograms.

## VI. CALIBAN PULSED REACTOR

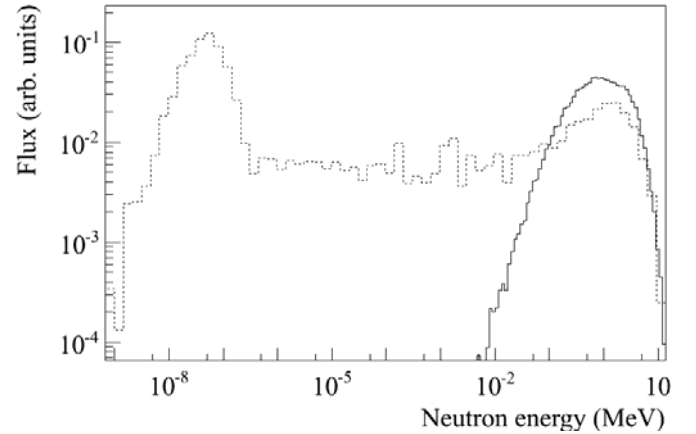


Fig. 6. Calculated CALIBAN neutron spectra in the central cavity (solid line) and outside the core between two polyethylene blocks (dashed). Spectra were calculated with the TRIPOLI 4.4 code [20].

The CALIBAN[13] pulsed reactor located at the CEA Valduc laboratory in France was chosen because it is able to deliver a neutron fluence of  $3 \times 10^{14} \text{ n.cm}^{-2}$  in a fast 60  $\mu\text{s}$  neutronic pulse. Moreover samples could be retrieved from the reactor cave after a cooling time of only 30 minutes. Up to two shots could be performed each day. The neutron spectrum inside the central cavity is a near fission spectrum with an average neutron energy of 1.44 MeV (see calculated spectra in Fig. 6.). For a typical 10  $\mu\text{g}$   $^{235}\text{U}$  sample, each shot would produce  $\sim 2 \times 10^7$  fission products and  $\sim 5 \times 10^6$  isomers. Irradiations were also done outside the core of the reactor where the sample was placed between two polyethylene blocks (each 1L in volume) to produce a more moderated neutron energy spectrum. The neutron spectra calculated

with the TRIPOLI 4.4 code [20] under this condition is shown as the dotted line in Fig. 6. This calculation yields a mean neutron energy of 0.29 MeV, and the neutron fluence is  $2.6 \times 10^{13}$  n.cm<sup>-2</sup> for a typical CALIBAN shot.

For most shots the neutron fluence was measured by co-activating indium foils placed in close proximity to the samples. As mentioned earlier, the  $^{115}\text{In}(n,n')^{115\text{m}}\text{In}$  reaction was used, measuring the 497 keV gamma line of  $^{115\text{m}}\text{In}$ . The reactor temperature rise  $\Delta T$  was also monitored for every shot to provide a measurement of the core heating which is directly related to the neutron fluence. The fluence ratios obtained from these two independent measurements  $\Delta T/\text{In}$  was determined to be constant with a rms deviation of 1%. Thus through many shots, the temperature rise in the reactor was calibrated to the In foil activation to provide an additional neutron fluence measurement that was ultimately used to determine the integral cross section leading to  $^{235\text{m}}\text{U}$ .

The integral fission and neutron capture cross sections given in Table IV, are calculated from the two CALIBAN neutron spectra shown in Fig. 6. and the latest ENDF/B-VII.1 cross sections [19]. These cross sections are relevant to the discussion presented in the background study section.

Isotope	Reaction	Integral cross section (barns)	
		Moderated spectrum $\langle E \rangle = 0.29$ MeV	Cavity spectrum $\langle E \rangle = 1.44$ MeV
$^{235}\text{U}$	n,f	303.5	1.25
$^{236}\text{U}$	n,f	0.17	0.37
$^{238}\text{U}$	n,f	0.04	-
$^{238}\text{U}$	n, $\gamma$	4.99	0.10

Table IV. Integral neutron-induced fission and capture cross sections for  $^{235}\text{U}$ ,  $^{236}\text{U}$ , and  $^{238}\text{U}$  corresponding to irradiations external to the reactor (moderated spectrum) or in the central-cavity (cavity spectrum) of CALIBAN. These cross sections were obtained by integrating the ENDF/B-VII.1 cross section over the neutron spectra shown in Fig. 6.

## VII. DATA ANALYSIS AND RESULT

An example electron decay curve measured with a  $^{235}\text{U}$  sample after a CALIBAN irradiation is shown in Fig. 7. The sample was dissolved off of the backing foil after the irradiation, the fission products were removed using the radiochemistry described earlier, then electrodeposited on a stainless steel disk and counted in the electron spectrometer. The data was fit with the following function:

$$f(t) = P_1 + P_2 e^{-\ln(2)t/T_{1/2}^{\text{iso}}} + P_3 e^{-\ln(2)t/T_{1/2}^{\text{bckg}}} \quad (4)$$

The first two terms are the same as given in Eq. 1 with the isomer half-life called out as  $T_{1/2}^{\text{iso}}$ . For these fits it was kept fixed to the measured value 25.62 minutes as given in Table

III. The third term is included to account for other activities that might be present in the sample, such as residual fission products, washed off Ti activation products or other backgrounds. To see how this third term would influence the fit, the  $P_3$  amplitude and the half-life  $T_{1/2}^{\text{bckg}}$  parameters were allowed to vary freely to obtain the best fit. This background activity could correspond to the decay of several isotopes so that the fitted values would represent an average of the ensemble. Attempts were made to fit the data with additional decay components beyond this third term, but no improvement in the reduced  $\chi^2$  was obtained and the isomer amplitude  $P_2$  was changed less than the  $P_2$  uncertainty given by the fit. Hence the three component function given by Eq. 4 was used throughout this work. The residue of the fit is shown in the upper part of Fig. 7. In this example the reduced  $\chi^2$  is 0.99. The background half-life when averaged over four shots is 1.7 minutes. In the fitting procedure, the first 30 second counting period was systematically removed due to the fast decrease of the dark current after the sample introduction. Sometimes a few minutes had to be removed to overcome this effect. This source of background could be clearly identified since it produces a non-exponential, much faster decay. A full discussion of the backgrounds is given in the next section.

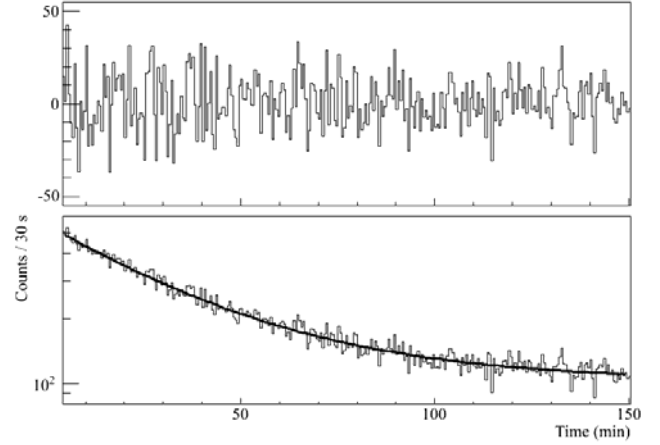


Fig. 7. An example decay curve (bottom) measured for an irradiated  $^{235}\text{U}$  sample after radiochemistry and electrodeposition. The solid line represents the fit to the data using the form given by Eq. 4. The residual between the data and the fit is shown in the top figure.

## VIII. BACKGROUND STUDY

As mentioned earlier, the only way the isomer can be identified is through its conversion electron decay half-life. The irradiation can produce other activities, such as fission products and activations from the backing material or impurities in the sample. Hence a careful study of all these background sources has been done. One concern is the possibility that other activities could be produced, which decay with a half-life (or composite half-life) that is close to

that of  $^{235m}\text{U}$  and thus could not be resolved in the decay time spectrum. To address this issue we performed additional irradiations with enriched samples of  $^{238}\text{U}$  and  $^{236}\text{U}$ , as well as with blank samples that contained no uranium. Table V summarizes the background half lives and amplitudes measured on  $^{235}\text{U}$ ,  $^{238}\text{U}$ ,  $^{236}\text{U}$  samples and on a Ti foil. They should be compared to the half-life and amplitude of the  $^{235m}\text{U}$  signal which are  $25.46 \pm 0.11$  minutes (held fixed) and  $1.20 \pm 0.01$  ( $\text{e}^- \cdot \mu\text{g}^{-1} \cdot \text{s}^{-1}$ ), respectively. No signal was observed for the Ti only blank. The small backgrounds measured on the uranium 236 and 238 samples are attributed to residual fission product decay.

Isotope	$T_{1/2}^{bckg}$ (min)	Amplitude ( $\text{e}^- \cdot \mu\text{g}^{-1} \cdot \text{s}^{-1}$ )
$^{235}\text{U}$	$1.70 \pm 0.24$	$0.2 \pm 0.3$
$^{238}\text{U}$	$3.4 \pm 1.4$	$0.3 \pm 0.2$
$^{236}\text{U}$	$18.4 \pm 1.3$	$0.4 \pm 0.2$
Ti blank	-	-

Table V. Averaged half-live and amplitudes for the  $^{235m}\text{U}$  isomer signal and possible backgrounds measured with a Ti blank and enriched samples of  $^{238}\text{U}$  and  $^{236}\text{U}$ .

An additional irradiation was made on a  $^{238}\text{U}$  sample in a moderated flux external to the reactor (see CALIBAN section) in order to have a high ratio (138/1) of capture to fission reaction rates. In this case neutron capture on  $^{238}\text{U}$  leads to the production of  $^{239}\text{U}$  which  $\beta$ - $\gamma$  decays with a half-life of  $23.45 \pm 0.02$  minutes [19] that is close to the isomer half-life. Since  $\beta$ - $\gamma$  decay also produces low-energy secondary electrons, this measurement provided a good test of our experimental setup, with a negligible background due to fission products decays. In a single shot, we measured a half-life of  $23.4 \pm 0.4$  minutes, which is in excellent agreement with the literature value. Only the first 30 s were removed in order to fit the decay curve, and a reduced  $\chi^2$  of 0.96 was obtained. This demonstrates the ability of the electron spectrometer to measure decays with good half-life determinations in the time range of interest, and for a signal amplitude ( $1.5 \text{ e}^- \cdot \mu\text{g}^{-1} \cdot \text{s}^{-1}$ ) on the same level as the  $^{235m}\text{U}$  isomer. This also demonstrates that the residual fission products decays are the only source of background in this experiment.

Hence for the final analysis on  $^{235}\text{U}$  samples the background half-life was kept fixed to the value measured with  $^{236}\text{U}$  at 18.4 minutes, which assumes that the background half-life originating from residual fission products is the same for  $^{236}\text{U}$  and  $^{235}\text{U}$ . This can be justified since the fission products yields do not vary significantly (5% on average over the whole mass distribution), and only the composite half-life is kept fixed. The amplitude of the background is still adjusted. Hence the associated uncertainty is considered to be negligible.

## IX. CROSS SECTION

The isomer integral cross section is calculated from the fitted  $P_2$  amplitude according to:

$$\sigma = 7.82 \times 10^{10} \times \frac{P_2 \times \tau_{iso} \times e^{t_{cool}/\tau_{cool}} \times e^{t_{chem}/\tau_{chem}}}{m \times \varepsilon(m) \times F} \quad (5)$$

where  $\tau_{iso}$  is the isomer lifetime (i.e.,  $\tau_{iso} = T_{1/2}/\ln(2)$ ),  $t_{cool}$  is the cooling (decay) time between the end of the irradiation and the beginning of the chemical separation,  $\tau_{cool} = 25.6 \pm 0.11$  minutes is the isomer lifetime for stippled samples,  $t_{chem}$  is the chemistry and electroplating duration,  $\tau_{chem}$  is the isomer lifetime when uranium is in solution (during chemistry and electro-deposition),  $m$  is the sample mass in micrograms measured by  $\alpha$  spectrometry for each sample,  $\varepsilon(m)$  is the electron detection efficiency given by Eq. 3 and  $F$  is the neutron fluence given in  $\text{n} \cdot \text{cm}^{-2}$  as obtained from the calibrated temperature rise of the reactor after the irradiation. Finally the cross section for the  $^{235}\text{U}$  isomer activation is obtained by averaging four  $^{235}\text{U}$  sample irradiations. The value of the integral  $^{235}\text{U}(n,n')^{235m}\text{U}$  cross section is:

$$1.00 \pm 0.13 \text{ barns.}$$

The uncertainty for each shot was obtained by propagating the different uncertainties in Eq. 5. Table VI gives the uncertainties averaged over the shots for all contributing parameters. The uncertainty related to the isomer half-life during chemistry and electro-deposition can not be measured. Hence we used an uncertainty of 10 % ( $\tau_{chem} = 25 \pm 2.5$  min), as mentioned earlier.

Parameter	Uncertainty (%)
Electron detection efficiency	7.7
Uncertainty on isomer half-life during cooling	0.43
Neutron flux measurement	4.7
$^{235}\text{U}$ mass measurement	3.2
Isomer $P_2$ amplitude	1
Isomer half-life during chemistry and electro-deposition	10
<b>Total uncertainty obtained by propagation in Eq. 5</b>	<b>13</b>

Table VI. Uncertainties associated with the determination of the integral cross section.

## X. CONCLUSION

The integral  $^{235}\text{U}(n,n')^{235m}\text{U}$  cross section has been measured in a fission-like neutron spectrum using the activation method. It has been obtained by irradiating several  $^{235}\text{U}$  samples in the pulsed critical assembly CALIBAN [13], and by counting the conversion electrons emitted in the isomer decay transition after radiochemical clean-up and electro-deposition. A careful study of background activities



was made and found to be small. Moreover, the influence of these backgrounds did not significantly change the isomer yield. Four isomer yield measurements were averaged to obtain a result of  $1.00 \pm 0.13$  barns. An evaluation performed with the TALYS-1.4 [8] code is presented in Fig. 8. (dotted curve). When averaged over the CALIBAN neutron energy spectrum, a value of 0.97 barns is obtained, in good agreement with our measurement.

In order to facilitate the discussion the experimental and theoretical (full curve) total inelastic cross section is also shown in Fig. 8. The integrated value of the evaluated total inelastic cross section is 1.66 barns. Hence the isomer production is calculated to exhaust 58 % of the total inelastic cross section. This value has to be compared to the most intense  $\gamma$  lines populated in the partial cross sections measurements reported in references [9] and [10], which are about 10 %. The partial cross section for the  $^{235m}\text{U}$  production is thus a very good constraint the total inelastic cross section. Since the present measurement is in agreement with the above evaluation, it supports that the measured total inelastic reported at low energies underestimate the total inelastic cross section. This is particularly true for the lowest energy point at 1 MeV [7], which coincides with the peak of isomer production cross section. This conclusion is emphasized since the highest sensitivity of our measurement is in the low energy part of excitation function where the CALIBAN neutron spectrum is peaked near 500 keV (see dash-dotted line in Fig. 8.).

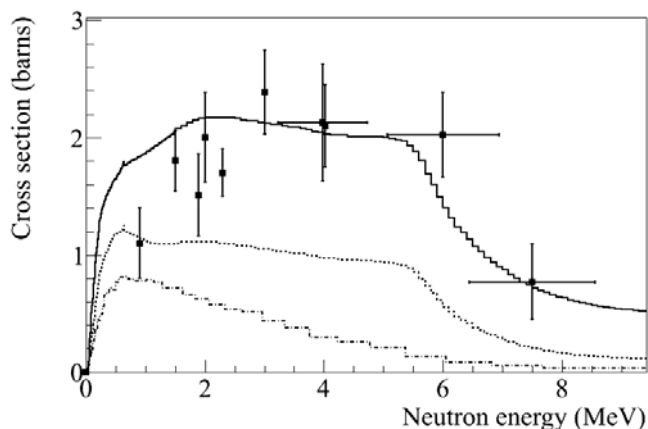


Fig. 8. Total neutron inelastic cross section data points taken from experiments [4,5,6,7] and a theoretical evaluation (full line), using TALYS-1.4 code [8]. The TALYS code was also used to calculate inelastic cross section leading to the population of the  $^{235m}\text{U}$  isomer (dashed line). The CALIBAN neutron spectrum is given by the dotted line.

## ACKNOWLEDGEMENTS

We would like to acknowledge the Valduc staff for their excellent performance in hosting us during this experiment.

This includes the operating crew of CALIBAN, the radiation technician support, and staff who assisted us with counting samples, setting up our counting equipment, and in assisting with the radiochemistry. We would also like to thank the GODIVA IV operating crew and staff who helped us during the radiochemical development test runs at Los Alamos National Laboratory.

The research was carried out under the US-France International Agreement on Cooperation on Fundamental Research Supporting Stockpile Stewardship. This work was performed under the auspices of the U.S. Department of Energy at Los Alamos National Laboratory operated by the Los Alamos National Security, LLC under Contract No. DE-AC52-06NA25396 and at Lawrence Livermore National Laboratory operated by the Lawrence Livermore National Security, LLC under Contract No. DE-AC52-07NA27344.

- [1] W.L. Talbert, Jr., J. W. Starner, R. J. Estep, S. J. Balestrini, M. Attrep, Jr., D. W. Efurud, and F. R. Roensch, Phys. Rev. C. 36, 1896 (1987); A. D'Eer, C. Wagemans, M. Nève de Mévergnies, F. Gönnerwein, P. Geltenbort, M. S. Moore, and J. Pauwels, Phys. Rev. C. 38, 1270 (1988).
- [2] J.E. Lynn and A.C. Hayes, Phys. Rev. C. 67, 014607 (2003).
- [3] V. Méot *et al.* CEA Report R-5944.
- [4] H. Knitter *et al.* Z. Phys. 257, 18 (1972).
- [5] R. Batchelor and K. Wyld, Report AWRE-O-55/69 (1969).
- [6] D.M. Drake Nuclear Physics A 133, 108(1969).
- [7] Andreev, V. N. Soviet Progress in Neutron Physics; authorized translation from the Russian. Edited by P. A. Krupchitskii. Published by Consultants Bureau, New York, 1963, p.211.
- [8] A. Koning, S. Hilaire, and M. Duijvestijn, in Proceedings of the International Conference on Nuclear Data for Science and Technology - ND2007 (EDP Sciences, Paris, France, 2008), pp. 211–214.
- [9] W. Younes *et al.* Lawrence Livermore National Laboratory report UCRL-ID-140313, US DOE, LLNL 2000.
- [10] M. Kerveno *et al.* Phys. Rev. C. 87, 024609 (2013).
- [11] M. Nève de Mévergnies and P. Del Marmol, Phys. Lett. B 49, 428 (1974).
- [12] M. Nève de Mévergnies, Phys. Rev. Lett. 29, 1188 (1972) ; V.V.Kol'tsov *et al.* Izvestiya Akademii Nauk SSSR S. Fiz. 53, 2085 (1989).
- [13] N. Authier and B. Mechtoua, "Bare, Highly Enriched Uranium, Fast Burst Reactor CALIBAN", ICSBEP Handbook, HMF-080 (2007).
- [14] E. P. Horwitz *et al.* Anal Chim. Acta. 266, 25 (1992).
- [15] E.M. Bond to be published.
- [16] R. Mostellar, "Godiva IV Delayed-Critical Experiments and an Associated Prompt-Burst Experiment," International Handbook of Evaluated Criticality Safety

---

Benchmark Experiments, NEA/NSC/DOC/(95)03/I, HEU-MET-FAST-086, 2012.

[17] E. M. Bond, T. A. Bredeweg, J. R. FitzPatrick, M. Jandel, R. S. Rundberg, A. K. Slemmons and D. J. Vieira, J. of Rad. and Nucl. Chem. 276, 549 (2008).

[18] A&M <http://www.am-fr.com>

[19] National Nuclear Data Center  
<http://www.nndc.bnl.gov/>

[20] TRIPOLI4.4 <http://www.oecd-neo.org/tools/abstract/detail/nea-1716/>